FULL PAPER

Dalton
www.rsc.org/dalton

Isomerization by ligand shuffling along a Cr_2^{4+} unit: further reactions leading to cleavage of a quadruple bond

Rodolphe Clérac,[a,b] F. Albert Cotton,*[a] Stephen P. Jeffery,[a] Carlos A. Murillo *[a] and Xiaoping Wang[a]

[a] *The Laboratory for Molecular Structure and Bonding, Department of Chemistry, Texas A&M University, PO Box 30012, College Station, TX 77842-3012, USA. E-mail: cotton@tamu.edu, murillo@tamu.edu*

[b] *Centre de Recherche Paul Pascal, CNRS UPR 8641, avenue du Dr. A. Schweitzer, 33600 Pessac, France*

Received 12th May 2003, Accepted 18th June 2003
First published as an Advance Article on the web 3rd July 2003

The paddlewheel complex $Cr_2(DpyF)_4$ (**1**), where DpyF = *N*,*N*′-di(2-pyridyl)formamidinate, has a short Cr–Cr distance of 1.938(2) Å for the Cr≡Cr quadruple bond. In solution, there is a series of interconverting isomers, as determined by variable temperature ^{1}H NMR studies. Compound **1** can be readily oxidized by $CuCl_2$ to produce $[Cr_2(DpyF)_4][CuCl_2]_2$ (**2**) and $[Cr_2(DpyF)_4CuCl_3][CuCl_2]$ (**3**). In both cases, the metal–metal quadruple bond is cleaved in favor of six-coordinate Cr(III) ions. Magnetic measurements for the oxidized products show that the chromium ions in the dichromium units exhibit strong antiferromagnetic interactions.

Introduction

Bidentate formamidinate ligands of general formula ArNCHNAr$^-$, where Ar are aryl groups (although there are alkyl groups in a few cases), have been successfully used in the synthesis of many dinuclear complexes with paddlewheel configuration, $M_2(ArNCHNAr)_4$ (**I**). This family of compounds, along with those of the type $M_2(carboxylate)_4$ and $M_2X_8^{n-}$, are among the best studied metal–metal-bonded complexes where the formal bond order can vary from ½ to 4.[1] Some of the appeal of $M_2(ArNCHNAr)_4$ complexes lies in the possibility of preparing them with a great variety of substituted aryl groups, which allow wide variation in the basicity of the ligands. This, in turn, affects intrinsic properties of the compounds, such as metal–metal distances and electrode potentials.[2] Further extension of the chemistry of metal–metal-bonded formamidinate ligands has been made recently by replacing the Ar substituents with one or two 2-pyridyl groups to generate potentially tridentate ligands such as *N*,*N*′-phenyl(2-pyridyl)formamidinate (PhpyF) (**II**)[3] and the potentially tetradentate ligand *N*,*N*′-di(2-pyridyl)formamidinate (DpyF) (**III**).[4] These have allowed the syntheses of the corresponding linear tri- and tetranuclear chromium complexes. For example, the trichromium compound $[Cr_3(DpyF)_4][PF_6]_2$ has an unsymmetrical structure with one short and one long separation between the three chromium atoms. The short Cr–Cr distance (~1.95 Å) corresponds to a Cr≡Cr quadruple bond, while the third chromium atom is isolated and in a distorted octahedral environment. The supporting DpyF ligands are arranged in a *trans* configuration and each metal atom is embraced by four approximately coplanar nitrogen atoms, leaving uncoordinated pyridyl N atoms in dangling positions. For the tetranuclear compound $[Cr_4(DpyF)_4Cl_2](PF_6)_2$, all the nitrogen atoms on the formamidinate ligands are coordinated to the metal centers, forming a linear chain with short–long–short separations between Cr atoms (**IV**).[4] A similar arrangement of the chromium chains has also been reported for di(2-pyridyl)amide (dpa) compounds of the type $Cr_3(dpa)_4X_2$ (X represents a monoanion).[5] In earlier work, it was found that the DpyF ligand is capable of forming dinuclear species with Mo_2^{4+} units.[6] In the solid state, the Mo_2 compound is very symmetrical, with each of the four bridging formamidinate ligands having a dangling pyridyl group at each end of the dimetal unit (**V**). However, in solution, the presence of all six possible isomers was evident from ^{1}H NMR studies. The isomers of **V** all rearranged back into the very symmetrical arrangement when the compound was crystallized and upon reaction with CuCl.

In this report, the results from a study of the Cr_2^{4+} system with DpyF are presented and the existence of several isomers for $Cr_2(DpyF)_4$ (**1**) shown by NMR spectroscopy. More importantly, variable temperature spectra are consistent with fluxionality that leads to isomer equilibration. This can be explained by sliding or shuffling[7] of formamidinate ligands along the Cr_2 unit. We also report the reactivity of **1** towards $CuCl_2$, which produces cleavage of the quadruple bond.

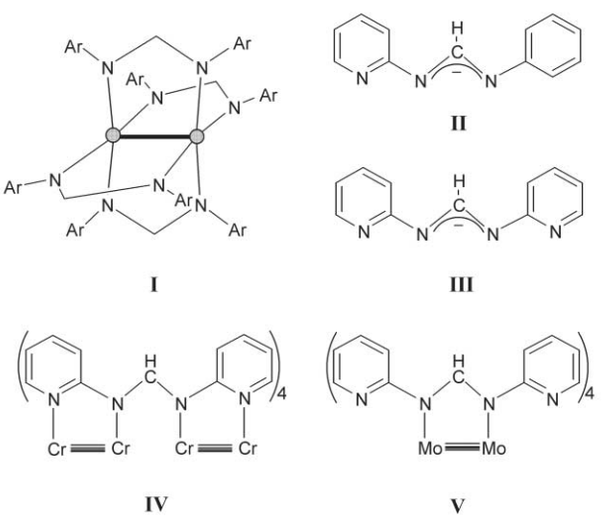

Experimental

General

Manipulations were performed under an atmosphere of argon using standard Schlenk techniques. Solvents were purified by conventional methods and were freshly distilled under nitrogen prior to use. Anhydrous $CrCl_2$ was purchased from Strem Chemicals, Inc. *N*,*N*′-di(2-pyridyl)formamidine (HDpyF) was prepared according to a published procedure.[8]

Physical measurements

^{1}H NMR spectra of **1** were recorded on a Varian UNITY Plus 300 instrument at 300 MHz, with chemical shifts being

DOI: 10.1039/b305304k

referenced to CD_2Cl_2 (δ 5.32 ppm). The electronic absorption spectra were measured on a Shimadzu UV-2501PC spectrophotometer. The magnetic susceptibility data in the solid state were collected on a Quantum Design MPMS-5 SQUID (superconducting quantum interference device) magnetometer from 2.0 to 300 K at a field of 1000 G. The magnetic susceptibility data were corrected for the sample holder contribution and for the intrinsic diamagnetic contribution calculated from Pascal's constants.[9] The electrochemical measurements were recorded on a BAS 100 electrochemical analyzer with Pt working and auxiliary electrodes, Ag/AgCl reference electrode, a scan rate of 100 mV sec^{-1}, and 0.1 M Bu_4NPF_6 (in CH_2Cl_2) as electrolyte. Under these experimental conditions, the $E_{½}(Fc^+/Fc)$ was measured at 440 mV. Elemental analyses were performed by Canadian Microanalytical Services, British Columbia, Canada.

Syntheses

$Cr_2(DpyF)_4$ (1). A solution of LiDpyF (0.82 g, 4.0 mmol) in THF (30 mL) was added to a Schlenk flask containing $CrCl_2$ (0.25 g, 2.0 mmol) at ambient temperature to give a red suspension. The reaction mixture was stirred and refluxed overnight to precipitate an orange solid. This solid was filtered and washed with methanol (15 mL)[10] and hexanes (15 mL). Yield: 0.74 g, 83%. Orange crystals of **1** were grown by dissolving the product in hot THF and layering with hexanes. Compound **1** is moisture and air sensitive. ^{1}H NMR (22 °C, CD_2Cl_2): δ 9.73 (s br, 4H, NC(H)N), 8.19 (m br, 8H, pyridyl), 7.39 (m br, 8H, pyridyl), 7.19 (m br, 8H, pyridyl), 6.63 (m br, 8H, pyridyl). IR (KBr, cm^{-1}): 1602 (s), 1576 (s), 1540 (s), 1487 (m), 1468 (m, sh), 1453 (s), 1429 (s), 1396 (m), 1336 (s, br), 1315 (m), 1298 (m), 1262 (w), 1243 (w), 1221 (s), 1158 (m), 1140 (w), 1022 (w), 981 (w), 943 (w), 851 (w), 836 (w), 788 (m), 776 (sh), 764 (m), 737 (m), 682 (w), 654 (w), 622 (w), 551 (w), 528 (w). UV/Vis [λ_{max}/nm (ε/M^{-1} cm^{-1})]: 480 (3060). $E_{½}$(ox): 700 mV. ESI-MS, *m*/*z* (calcd.) for $[M + 2H]^{2+}$: 446.09 (446.10). Anal. calcd. for $C_{44}H_{36}Cr_2N_{16}$: C, 59.19; H, 4.06; N, 25.10; found: C, 58.94; H, 4.11; N, 25.17%.

$[Cr_2(DpyF)_4][CuCl_2]_2\cdot CH_3CN$ ($2\cdot CH_3CN$). Acetonitrile (20 mL) was added into a Schlenk flask containing a mixture of **1** (0.18 g, 0.20 mmol) and $CuCl_2$ (0.060 g, 0.45 mmol) at ambient temperature to give immediately a yellow suspension. The reaction mixture was stirred for about 4 h until an orange solution having a small amount of a suspended solid was formed. After filtration, the solution was layered with diethyl ether. Orange–red colored crystals of $2\cdot CH_3CN$ were obtained in one week. Yield: 0.19 g, 79%. IR (KBr, cm^{-1}):1628 (s), 1599 (s), 1581 (sh), 1560 (vs), 1468 (s), 1448 (m), 1430 (m), 1406 (w), 1374 (s), 1310 (m), 1299 (m), 1239 (s), 1161 (w), 1027 (w), 991 (w), 952 (w), 839 (w), 779 (m), 772 (m), 739 (m), 658 (w), 497 (w), 434 (w). UV/Vis [λ_{max}/nm (ε/M^{-1} cm^{-1})]: 533 (340), 741 (30). Anal. calcd. for $C_{46}H_{39}Cr_2Cu_2N_{17}Cl_4$: C, 45.93; H, 3.27; N, 19.80; found: C, 45.70; H, 3.34; N, 19.82%.

$[Cr_2(DpyF)_4][CuCl_2]_2\cdot 2(CH_3)_2CO$ [$2\cdot 2(CH_3)_2CO$]. Acetone (30 mL) was added into a Schlenk flask containing a mixture of **1** (0.09 g, 0.10 mmol) and $CuCl_2$ (0.030 g, 0.22 mmol) at ambient temperature. The yellow suspension was refluxed for about 6 h, giving an orange solution with a small amount of solid. It was then filtered and the filtrate was layered with diethyl ether. Red crystals of $2\cdot 2(CH_3)_2CO$ were obtained in two weeks. Yield: 0.07 g, 58%. IR (KBr, cm^{-1}): 1648 (w), 1628 (m), 1582 (m), 1570 (s), 1466 (s), 1448 (m), 1430 (m), 1375 (s), 1310 (m), 1298 (m), 1240 (m), 1161 (m), 1028 (m), 952 (m), 839 (w), 770 (m), 738 (w), 658 (w), 498 (m), 435 (s), 408 (s). UV/Vis [λ_{max}/nm (ε/M^{-1} cm^{-1})]: 532 (300), 737 (36). The crystals were dried under vacuum to remove the interstitial acetone molecules for elemental analysis. Anal. calcd. for $C_{44}H_{36}Cr_2Cu_2N_{16}Cl_4$: C, 45.49; H, 3.12; N, 19.29; found: C, 45.05; H, 3.20; N, 19.39%.

$[Cr_2(DpyF)_4(CuCl_3)][CuCl_2]\cdot CH_3CN$ ($3\cdot CH_3CN$). Reaction of a molar excess of $CuCl_2$ (0.10 g, 0.74 mmol) and a lesser molar amount of **1** (0.16 g, 0.19 mmol) in acetonitrile (20 mL) was carried out similarly to that above. After layering the solution with diethyl ether, two types of red crystals were obtained. Dark red-colored crystals of $3\cdot CH_3CN$ were separated by hand from the red crystals of $2\cdot CH_3CN$. Yield: 0.14 g, 60%. IR (KBr, cm^{-1}): 1612 (s), 1598 (s), 1552 (vs), 1527 (m), 1492 (m), 1472 (s), 1446 (sh, m), 1430 (s), 1358 (s), 1336 (sh, m), 1294 (s), 1252 (s), 1184 (w), 1166 (w), 1026 (w), 988 (w), 970 (w), 954 (w), 783 (m), 740 (w), 658 (w), 497 (w), 434 (m). UV/Vis [λ_{max}/nm (ε/M^{-1} cm^{-1})]: 533 (270), 741 (30). Anal. calcd. for $C_{46}H_{39}Cr_2Cu_2N_{17}Cl_5$: C, 44.62; H, 3.17; N, 19.23; found: C, 44.56; H, 3.12; N, 19.23%.

Crystallography

Each crystal was mounted on a quartz fiber with a small amount of silicone grease and transferred to a goniometer head. Geometric and intensity data for **1** at 213 K were gathered on a Nonius FAST area detector system, utilizing the software program MADNES.[11] Cell parameters for FAST data were obtained from an auto-indexing routine and were refined with 250 strong reflections in the 2θ range 18.1–41.6°. Cell dimensions and Laue symmetry for all crystals were confirmed from axial photographs. All data were corrected for Lorentz and polarization effects. Intensity data were transferred into SHELX format using the program PROCOR.[12] Data for $2\cdot CH_3CN$, $2\cdot 2(CH_3)_2CO$ and $3\cdot CH_3CN$ at 213 K were collected on a Bruker AXS SMART 1000 CCD system equipped with a liquid nitrogen low temperature controller. For each of the four data sets, the majority of the atomic positions were found by the direct methods program in the SHELXTL software package. Subsequent cycles of least-squares refinement followed by difference-Fourier syntheses revealed the positions of remaining non-hydrogen atoms. Hydrogen atoms were placed in calculated positions. Crystal data and structural refinement information for **1**, $2\cdot CH_3CN$, $2\cdot 2(CH_3)_2CO$ and $3\cdot CH_3CN$ are given in Table 1.

CCDC reference numbers 206653–206656.

See http://www.rsc.org/suppdata/dt/b3/b305304k/ for crystallographic data in CIF or other electronic format.

Results and discussion

$Cr_2(DpyF)_4$ (1)

Reaction of $CrCl_2$ with LiDpyF using a 1 to 2 molar ratio in THF yields **1** (eqn. 1) as an orange precipitate. This appears to be chemically pure as shown by mass spectroscopy. But, as discussed below, the solid so obtained appears to be composed of a mixture of isomers.

$$2CrCl_2 + 4LiDpyF \xrightarrow[\Delta]{THF} Cr_2(DpyF)_4 + 4LiCl \qquad (1)$$

Crystallization was very difficult, as many attempts generated only powdery solids. However, slow diffusion of hexanes into a dilute solution of the orange solid in THF provided single crystals. Diffraction experiments showed that these belong to the triclinic space group $P\bar{1}$ and have the composition $Cr_2(DpyF)_4$, with the molecule residing on a general position. A view of the molecule is shown in Fig. 1, with selected bond distances and angles given in Table 2. The most striking feature is the highly unsymmetrical arrangement of the four formamidinate ligands. One of the bridging ligands binds the Cr_2 unit using the formamidine [*N*C(H)*N*] nitrogen atoms, while the others use formamidinate and pyridyl N atoms. For the latter, the dangling nitrogen atoms point in one direction for two of the bridging ligands and in the opposite direction for the other, as shown schematically in **VI**. This arrangement, which is one of the

Table 1 Crystallographic data for **1**, **2**·CH_3CN, **2**·2$(CH_3)_2CO$ and **3**·CH_3CN

Compound	**1**	**2**·CH_3CN	**2**·2$(CH_3)_2CO$	**3**·CH_3CN
Formula	$C_{44}H_{36}Cr_2N_{16}$	$C_{46}H_{39}Cr_2Cu_2N_{17}Cl_4$	$C_{50}H_{48}Cr_2Cu_2N_{16}O_2Cl_4$	$C_{46}H_{39}Cr_2Cu_2N_{17}Cl_5$
M	892.89	1202.82	1277.92	1238.27
T/K	213	213	213	213
Space group	$P\bar{1}$	$P\bar{1}$	$P\bar{1}$	$P\bar{1}$
a/Å	11.960(3)	8.907(1)	8.5393(7)	10.5665(5)
b/Å	13.305(3)	14.005(2)	17.374(1)	12.8413(7)
c/Å	13.510(5)	20.237(3)	18.760(2)	18.949(1)
α/°	66.75(2)	92.957(2)	94.327(2)	86.269(1)
β/°	89.96(5)	97.270(2)	96.490(2)	75.518(1)
γ/°	88.52(4)	90.847(2)	95.157(2)	80.250(1)
U/Å^3	1974(1)	2500.2(5)	2743.9(4)	2452.8(2)
Z	2	2	2	2
D_{calc}/g cm^{-3}	1.502	1.598	1.547	1.677
R indices [$I>2\sigma(I)$]: $R1$,[a] $wR2$[b]	0.080, 0.153	0.035, 0.092	0.061, 0.135	0.041, 0.096
R indices (all data): $R1$,[a] $wR2$[b]	0.121, 0.173	0.047, 0.099	0.097, 0.155	0.064, 0.106

[a] $R1 = \Sigma||F_o| - |F_c||/\Sigma|F_o|$. [b] $wR2 = \{\Sigma[w(F_o^2 - F_c^2)^2]/\Sigma[w(F_o^2)^2]\}^{1/2}$, $w = 1/[\sigma^2(F_o^2) + (aP)^2 + bP]$, where $P = [\max(0 \text{ or } F_o^2) + 2(F_c^2)]/3$.

Table 2 Selected bond distances (Å) and angles (°) for $Cr_2(DpyF)_4$ (**1**)

Cr(1)–Cr(2)	1.938(2)	Cr(2)–N(2)	2.032(6)
Cr(1)–N(3)	2.083(6)	Cr(2)–N(6)	2.052(6)
Cr(1)–N(5)	2.073(6)	Cr(2)–N(9)	2.065(6)
Cr(1)–N(10)	2.061(6)	Cr(2)–N(13)	2.058(6)
Cr(1)–N(14)	2.066(6)		
N(3)–Cr(1)–N(5)	169.0(2)	N(2)–Cr(2)–N(6)	172.6(2)
N(3)–Cr(1)–N(10)	90.6(2)	N(2)–Cr(2)–N(9)	90.5(2)
N(3)–Cr(1)–N(14)	92.7(2)	N(2)–Cr(2)–N(13)	88.9(2)
N(5)–Cr(1)–N(10)	88.5(2)	N(6)–Cr(2)–N(9)	89.9(2)
N(5)–Cr(1)–N(14)	86.9(2)	N(6)–Cr(2)–N(13)	89.2(2)
N(10)–Cr(1)–N(14)	172.6(3)	N(9)–Cr(2)–N(13)	168.9(3)

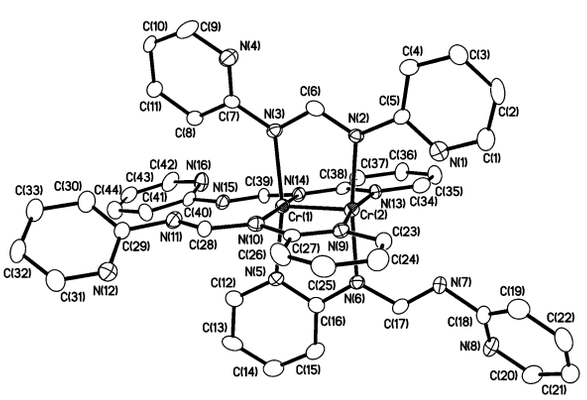

Fig. 1 Perspective view of the molecule of **1**. Atoms are drawn at the 40% probability level. Hydrogen atoms are omitted for clarity.

least symmetrical of various possible isomers (see below), contrasts with the highly symmetrical distribution of the bridging ligands in crystalline $Mo_2(DpyF)_4$ (**V**), where all four ligands bind to the Mo_2 unit using only the formamidine N atoms, leaving a pyridyl group dangling at each end of the dimetal unit.

The Cr–Cr distance of 1.938(2) Å is in the range of supershort Cr≡Cr quadruple bonds.[1m] It is only slightly longer than those in other Cr_2(formamidinate)$_4$ compounds without axial interactions, which are in the range 1.905–1.930 Å, but considerable longer than that of 1.87 Å in **VII**,[13] where the ligand binding through a pyridyl and an amide group resembles that found in the unsymmetrically bridged ligands of **1**.

There are also three relatively long axial interactions of ~2.93 Å to free formamidinate N atoms in the unsymmetrically bridging ligands. Although they are weak, it has been shown before that such interactions can have an important impact in the length of the Cr–Cr bond.[14]

The obvious question that arises by looking at the solid state structure is whether it remains intact in solution. Since the compound is diamagnetic, proton NMR spectroscopy is an appropriate tool. At room temperature there are only 5 signals, but they are all relatively broad and devoid of fine structure. There is only one methine signal [NC(*H*)N] at 9.73 ppm. The other four peaks are at 8.19, 7.39, 7.19 and 6.63 ppm, and can be assigned to the pyridyl H atoms. These appear to be consistent with a symmetrical structure, since methine protons in the symmetrical and unsymmetrical bridging modes are expected to produce signals with very different chemical shifts. However, the broadness of the signals at room temperature does not permit the simple conclusion that the compound rearranges to a symmetrical state upon dissolution of the crystals. It suggests that there are some other processes taking place.

Variable temperature data, shown in Fig. 2, show that as the temperature is lowered, the methine signal broadens even more and then splits into multiple peaks with δ values of 10.55, 10.22, 9.68 and 9.59 at −77 °C. Changes also occur in the pyridyl signals. We take this as evidence of the existence of interconverting isomers at ambient temperature. This evidence is stronger but complements that provided in a previous study on the $Mo_2(DpyF)_4$ system, in which we also proposed the existence of isomers in equilibrium.[6] In that study, it was concluded that dissolution of one single crystal of the symmetrical isomer produced at least six isomers in solution at room temperature, as determined from the presence of six methine signals in the NMR spectrum. A discussion of the various isomers (see Chart 1) was provided there and need not be repeated here.

The most important implication of the easy interconvertibility of various isomers in $M_2(DpyF)_4$ (M = Cr, Mo) compounds is that the ligands can move along the M_2 unit with

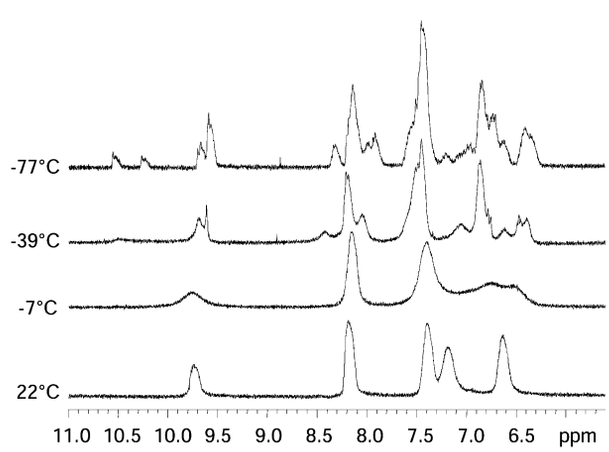

Fig. 2 Variable temperature ^{1}H NMR spectra for **1** in CD_2Cl_2 solution. The DpyF ligand methine [NC(*H*)N] signals appear in the range 10.6 to 9.5 ppm. The remaining signals are from the ligand pyridyl *H* atoms.

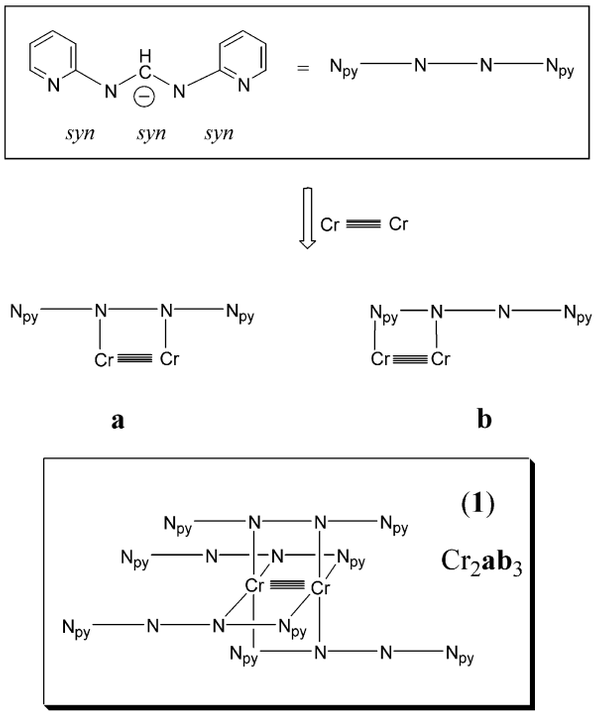

Chart 1

relative ease. The details of the exchange process are not known, but shuffling of the ligand along the M≡M bond may well be aided by axial interactions of the metal centers to the "free" nitrogen atoms in a manner similar to that shown in an earlier study of $Cr_2(DphIP)_4$ [**VIII**; DphIP = the anion of 2,6-di(phenylimino)piperidine].[14]

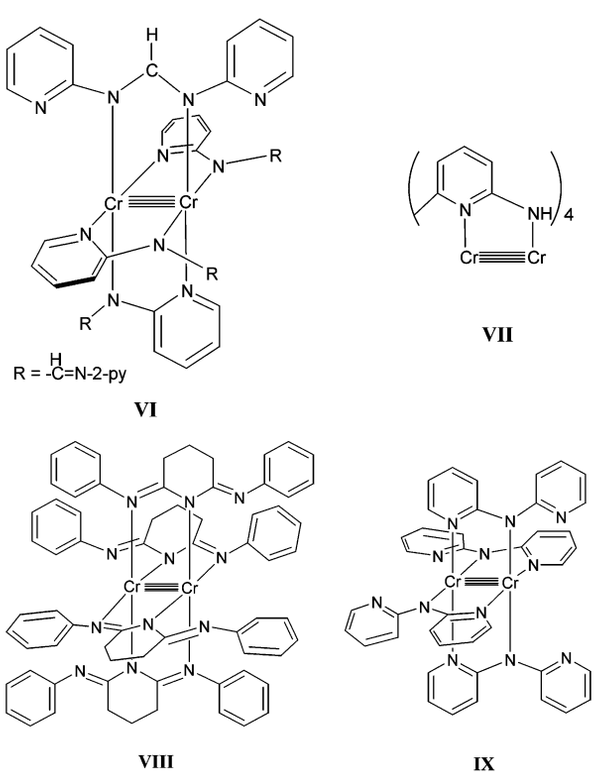

The shuffling of ligands appears to be an important process when ligands possessing extra nitrogen donor atoms are present, as in $Cr_2(dpa)_4$ (**IX**).[15] Here, the dpa anions arrange symmetrically about the Cr_2 unit with two dangling pyridyl groups on each end. This compound reacts with Cr(II) to give a linear trinuclear unit of the type $Cr_3(dpa)_4X_2$, where all nitrogen atoms are bound to the metal centers in a process that evidently requires shuffling of the ligands.[5] Likewise, addition of CuCl to a mixture of isomers of $Mo_2(DpyF)_4$ produced a single isomer of a compound that is symmetrical.

The shuffling of ligands on metal–metal-bonded units in solution, perhaps more slowly than in the molybdenum analog, suggests that the solid $Cr_2(DpyF)_4$, initially obtained from the reaction is likely to be a mixture of isomers, and this is probably why crystallization was so difficult to achieve.

$[Cr_2(DpyF)_4][CuCl_2]_2$ (2)

Compound **1**, like most Cr_2 paddlewheel, complexes displays an irreversible oxidation wave at $E_{1/2}(ox) = +0.70$ V *vs.* Ag/AgCl in the range +1.3 to −1.5 V. The irreversible nature of the oxidation process indicates a significant change in the coordination geometry of the chromium ions upon oxidation. Therefore, the reactivity of **1** towards the mild oxidizing agent $CuCl_2$ was studied, and a two electron oxidized product $[Cr_2(DpyF)_4][CuCl_2]_2$ (**2**) (eqn. 2) was obtained. The yield of **2** is essentially quantitative when the reaction is performed in acetonitrile. The product is isolated as a crystalline solvate, **2**·CH_3CN, after layering the reaction solution with diethyl ether. However, when the reaction is performed in acetone, it produces **2**·$2(CH_3)_2CO$ in much lower yield, probably due to the decreased solubility of both the starting material and product in acetone.

$$Cr_2(DpyF)_4 + 2CuCl_2 \xrightarrow[\Delta]{CH_3CN \text{ or acetone}} [Cr_2(DpyF)_4][CuCl_2]_2 \quad (2)$$

Compound **2**·CH_3CN crystallizes in triclinic space group $P\bar{1}$ with the cation and anions residing on general positions. The structure of the cation in **2**·CH_3CN is shown in Fig. 3. Selected bond distances and angles are listed in Table 3. There are four nitrogen donor atoms on each DpyF ligand available as potential coordination sites, two from the pyridyl groups and the other two from the central formamidine group. In **2**, each DpyF ligand uses a pair of adjacent pyridyl and formamidine N donor atoms to chelate one chromium atom, while the second formamidine nitrogen atom coordinates to the other chromium. The second N atom on the other pyridyl group is not used for coordination. The position of the second formamidine nitrogen atom alternates around the Cr ··· Cr vector, giving an idealized S_4 type arrangement, if the rotational orientations of the dangling pyridyl groups are ignored. The two Cr atoms are separated by a distance of 3.4192(6) Å. A similar structural motif has also been found in **2**·$2(CH_3)_2CO$, where the Cr ··· Cr

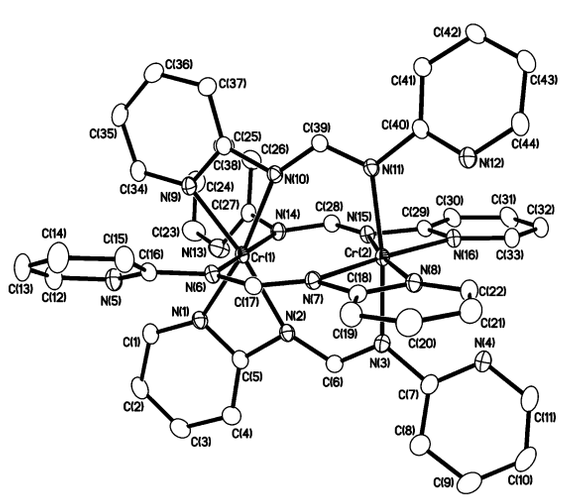

Fig. 3 Perspective view of the $[Cr_2(DpyF)_4]^{2+}$ cation in **2**·CH_3CN. Atoms are drawn at the 40% probability level. Hydrogen atoms are omitted for clarity.

Table 3 Selected bond distances (Å) and angles (°) for **2**·CH_3CN and **2**·$2(CH_3)_2CO$

	2·CH_3CN	**2**·$2(CH_3)_2CO$
Cr(1)–Cr(2)	3.4192(6)	3.408(1)
Cr(1)–N(1)	2.032(2)	2.031(4)
Cr(1)–N(2)	2.100(2)	2.119(4)
Cr(1)–N(6)	2.046(2)	2.044(4)
Cr(1)–N(9)	2.027(2)	2.030(4)
Cr(1)–N(10)	2.128(2)	2.133(4)
Cr(1)–N(14)	2.033(2)	2.037(4)
Cr(2)–N(3)	2.034(2)	2.051(4)
Cr(2)–N(7)	2.137(2)	2.131(4)
Cr(2)–N(8)	2.027(2)	2.027(5)
Cr(2)–N(11)	2.048(2)	2.044(4)
Cr(2)–N(15)	2.122(2)	2.115(5)
Cr(2)–N(16)	2.024(2)	2.032(4)
N(1)–Cr(1)–N(2)	64.70(7)	64.26(16)
N(1)–Cr(1)–N(9)	105.72(7)	104.94(17)
N(2)–Cr(1)–N(10)	125.48(7)	126.70(16)
N(6)–Cr(1)–N(14)	171.86(7)	171.90(17)
N(9)–Cr(1)–N(10)	64.09(7)	64.10(16)
N(3)–Cr(2)–N(11)	172.49(7)	172.28(17)
N(7)–Cr(2)–N(8)	64.09(7)	64.14(17)
N(7)–Cr(2)–N(15)	125.50(7)	125.71(17)
N(8)–Cr(2)–N(16)	106.32(7)	106.04(18)
N(15)–Cr(2)–N(16)	64.11(7)	64.13(17)

separation is 3.408(1) Å. The structure of the cation in **2** can be compared to that of **1**, where a short Cr–Cr distance of 1.938(2) Å was found. In **2**, each of the chromium atoms is six-coordinate. There is no direct bonding interaction between the two chromium atoms. The remote possibility that the two electron oxidation of the quadruply bonded Cr_2^{4+} core in **1** could have generated a triply bonded Cr_2^{6+} product did not come into play because of the additional nitrogen atoms on the DpyF ligands available for coordination and the strong tendency of Cr(III) to have octahedral coordination. The formation of four additional Cr–N bonds in **2** provides energetic compensation for the loss of Cr–Cr bonding, whereas in **1**, each Cr(II) atom is coordinated by only four nitrogen atoms, in accord with its being subject to Jahn–Teller distortion, and retention of the Cr–Cr quadruple bond is favored. This type of competition (ligand–metal *vs*. metal–metal bonding) has been reported for some other dinuclear complexes, examples being the two d^3 V(II) ions in $V_2(dpa)_4$[16] and the nickel atoms in $Ni_2(PhpyF)_4$.[3]

$[Cr_2(DpyF)_4(CuCl_3)][CuCl_2]$ (3)

Compound **3** was first isolated by serendipity when a slight excess of $CuCl_2$ was used in the preparation of **2**. A mixture of **2** and **3** was obtained, and both crystallized as acetonitrile solvates. Crystals of **2**·CH_3CN are orange–red while crystals of **3**·CH_3CN are dark red in color. Their distinct crystal morphologies make it possible to separate them manually. Compound **3** crystallizes in triclinic space group $P\bar{1}$ as dark red blocks. Selected bond distances and angles are listed in Table 4. A structure of the cation in **3**·CH_3CN is shown in Fig. 4. In the cation, there are two Cr(III) atoms with coordination geometry similar to that observed for **2**. The Cr ··· Cr separation of 3.3445(6) Å is consistent with the cleavage of the Cr≡Cr quadruple bond after oxidation. The Cr–N distances for the six-coordinated Cr(III) ions range from 2.014(3) to 2.128(3) Å. Instead of the two Cu(I) anions, namely $[CuCl_2]^-$, found in **2**, there is only one Cu(I) anion found in **3**. The other anion is $[CuCl_3]^-$, which has a Cu(II) ion coordinated directly to one of the pyridyl nitrogen atoms. The Cu(II) ion adopts an overall distorted tetrahedral geometry. A higher yield (60%) synthesis of **3** can be achieved when a stoichiometric molar ratio of 2 to 3 is used for the reaction of $Cr_2(DpyF)_4$ with $CuCl_2$ in acetonitrile.

Table 4 Selected bond distances (Å) and angles (°) for **3**·CH_3CN

Cr(1)–N(3)	2.128(3)	Cr(2)–N(2)	2.060(3)
Cr(1)–N(4)	2.037(2)	Cr(2)–N(5)	2.051(2)
Cr(1)–N(7)	2.027(3)	Cr(2)–N(6)	2.123(3)
Cr(1)–N(10)	2.123(2)	Cr(2)–N(9)	2.050(3)
Cr(1)–N(11)	2.014(3)	Cr(2)–N(14)	2.034(2)
Cr(1)–N(16)	2.045(2)	Cr(2)–N(15)	2.126(2)
Cu(1)–N(1)	2.050(3)	Cu(1)–Cl(3)	2.266(1)
Cu(1)–Cl(1)	2.251(1)	Cu(2)–Cl(4)	2.094(1)
Cu(1)–Cl(2)	2.2231(9)	Cu(2)–Cl(5)	2.094(1)
N(4)–Cr(1)–N(3)	64.04(9)	N(9)–Cr(2)–N(2)	172.64(9)
N(10)–Cr(1)–N(3)	127.90(9)	N(5)–Cr(2)–N(6)	63.86(9)
N(11)–Cr(1)–N(4)	104.0(1)	N(14)–Cr(2)–N(5)	104.7(1)
N(11)–Cr(1)–N(10)	64.01(9)	N(6)–Cr(2)–N(15)	127.52(9)
N(7)–Cr(1)–N(16)	174.0(1)	N(14)–Cr(2)–N(15)	63.95(9)
N(1)–Cu(1)–Cl(2)	146.19(8)	Cl(1)–Cu(1)–Cl(3)	136.54(4)
N(1)–Cu(1)–Cl(1)	95.16(8)	Cl(2)–Cu(1)–Cl(3)	100.83(3)
N(1)–Cu(1)–Cl(3)	90.28(8)	Cl(5)–Cu(2)–Cl(4)	175.65(5)
Cl(2)–Cu(1)–Cl(1)	98.15(4)		

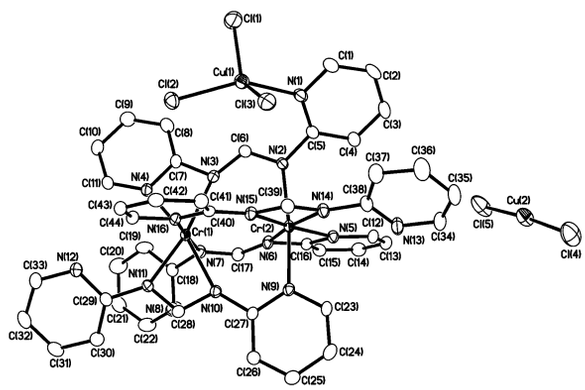

Fig. 4 Perspective view of **3**·CH_3CN. Atoms are drawn at the 40% probability level. Hydrogen atoms are omitted for clarity

Magnetic studies

As shown in Fig. 5, χT for **3** (open circles) decreases rapidly with temperature from 1.8 emu K mol^{-1} at 300 K to a value of 0.39 emu K mol^{-1} at 25 K. At lower temperatures, χT is constants then finally decreases slightly to reach 0.34 emu K mol^{-1} at 1.8 K. This feature is indicative of paramagnetic centers coupled by strong antiferromagnetic interactions. Based on the structure analyzed above, complex **3** can be described magnetically by Chart 2.

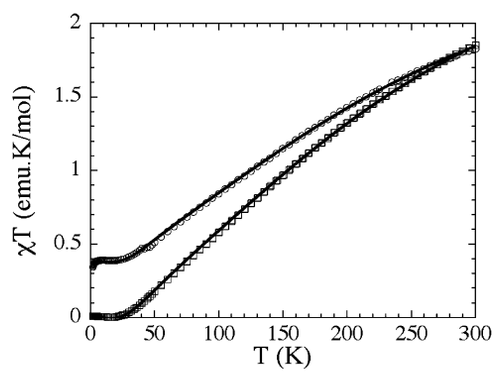

Fig. 5 Temperature dependence of the χT product for **2** (□) and **3** (○). The solid lines represent the best fits obtained with a dimer model of $S = \frac{3}{2}$ magnetic spins for **2** and with a dimer model of $S = \frac{3}{2}$ magnetic spins for the Cr_2(III,III) core, in addition to a Curie law of $S = ½$ for the Cu(II) center, for **3**.

The magnetic coupling between Cr(2) and Cu(1) through the N(2)–C(5)–N(1) bridge is most likely very weak and has been neglected (*i.e.*, $j = 0$) as a first approximation in the model.

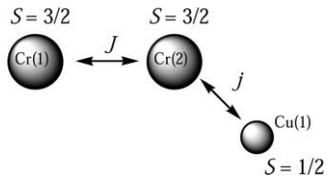

Chart 2

Therefore, this system can be described magnetically as a dimer of Cr(III) $S = \frac{3}{2}$ spins and an isolated $S = ½$ (for the Cu(II) site), which should follow a Curie law. Hence, the following equation for the magnetic susceptibility was used to fit the data:

$$\chi = \frac{N{g_{Cr}}^2{\mu_B}^2}{k_B T}\left\{\frac{2\exp\left(\frac{2J}{k_B T}\right)+10\exp\left(\frac{6J}{k_B T}\right)+28\exp\left(\frac{12J}{k_B T}\right)}{1+3\exp\left(\frac{2J}{k_B T}\right)+5\exp\left(\frac{6J}{k_B T}\right)+7\exp\left(\frac{12J}{k_B T}\right)}\right\}+ \frac{N{g_{Cu}}^2{\mu_B}^2}{4k_B T}+\chi_{dia} \quad (3)$$

where N, m_B and k_B, have their usual meanings, g_{Cr} and g_{Cu} are the Landé factors of the Cr(III) and Cu(II) sites, respectively, and J is the magnetic exchange constant between the Cr(III) ions ($S = \frac{3}{2}$) in the dimer considering the Hamiltonian $\boldsymbol{H} = -2J(S_{Cr1} \cdot S_{Cr2})$. Fitting of the data (solid line on Fig. 5) with the previous expression leads to $J/k_B = -66$ K and typical values for the g factors: $g_{Cr} = 2.02$, $g_{Cu} = 2.13$. Attempts were made to include a non-zero value for j [magnetic exchange between Cu(II) and Cr(III)] in the model, but the fitting of the data was not significantly improved. As expected, j is most likely very small, of the order of tenths of Kelvin, and cannot be accurately estimated. It is worth noting that the decrease in χT below 5 K is probably due to weak antiferromagnetic interaction between trinuclear units. Magnetic measurements performed on **2** reveal a behavior similar to that of **3**; the χT product decreases strongly with temperature between 300 and 25 K from 1.84 emu K mol^{-1} to a value close to zero, indicative of a diamagnetic ground state (open squares in Fig. 5). In view of the structure of **2**, a simple dimer model with $S_1 = S_2 = ½$ was used to fit the magnetic susceptibility (first part of eqn. 3). The best set of parameters obtained using this model was found to be $J/k_B = -65$ K and $g_{Cr} = 2.06$. As expected, based on the almost identical geometry of the dimeric Cr(III) unit in **3** and **2**, the g and J parameters are very similar in both compounds. These values are consistent with those obtained for other dinuclear Cr(III) compounds.[10,17]

References and notes

1 (*a*) F. A. Cotton, C. A. Murillo and I. Pascual, *Inorg. Chem.*, 1999, **38**, 2182; (*b*) K. M. Carlson-Day, J. L. Eglin, L. T. Smith and R. J. Staples, *Inorg. Chem.*, 1999, **38**, 2216; (*c*) K. M. Carlson-Day, J. L. Eglin, C. Lin, L. T. Smith, R. J. Staples and D. O. Wipf, *Polyhedron*, 1999, **18**, 817; (*d*) T. Ren, *Coord. Chem. Rev.*, 1998, **175**, 43; (*e*) C. Lin, T. Ren, E. J. Valente and J. D. Zubkowski, *J. Chem. Soc., Dalton Trans.*, 1998, 571; (*f*) F. A. Cotton, L. M. Daniels, X. J. Feng, D. J. Maloney, J. H. Matonic and C. A. Murillo, *Inorg. Chim. Acta*, 1997, **256**, 291; (*g*) F. A. Cotton, J. H. Matonic and C. A. Murillo, *Inorg. Chim. Acta*, 1997, **264**, 61; (*h*) F. A. Cotton, L. M. Daniels, J. H. Matonic and C. A. Murillo, *Inorg. Chim. Acta*, 1997, **256**, 277; (*i*) A. Singhal and V. K. Jain, *Can. J. Chem.*, 1996, **74**, 2018; (*j*) F. A. Cotton, L. M. Daniels and C. A. Murillo, *Inorg. Chem.*, 1993, **32**, 2881; (*k*) F. A. Cotton and T. Ren, *J. Am. Chem. Soc.*, 1992, **114**, 2495; (*l*) J. L. Bear, C. L. Yao, R. S. Lifsey, J. D. Korp and K. M. Kadish, *Inorg. Chem.*, 1991, **30**, 336; (*m*) F. A. Cotton and R. A. Walton, *Multiple Bonds Between Metal Atoms*, Clarendon Press, Oxford, 2nd edn., 1993 and references therein.

2 See for example: C. Lin, J. D. Protasiewicz, E. T. Smith and T. Ren, *Inorg. Chem.*, 1996, **35**, 6422.

3 F. A. Cotton, P. Lei and C. A. Murillo, *Inorg. Chim. Acta*, 2003, **349**, 173.

4 F. A. Cotton, L. M. Daniels, C. A. Murillo and X. Wang, *Chem. Commun.*, 1998, 39.

5 F. A. Cotton, L. M. Daniels, C. A. Murillo and I. Pascual, *J. Am. Chem. Soc.*, 1997, **119**, 10 223.

6 R. Clérac, F. A. Cotton, K. R. Dunbar, C. A. Murillo and X. Wang, *Inorg. Chem.*, 2001, **40**, 420.

7 M. H. Chisholm, D. L. Clark and M. J. Hampden-Smith, *J. Am. Chem. Soc.*, 1989, **111**, 574 . The term "shuffle" was used in reference to the so-called "Bloomington shuffle.".

8 H. Remlinger, W. R. F. Lingier, J. J. M. Vandewalle and R. Merényi, *Chem. Ber.*, 1971, **104**, 3965.

9 *Theory and Applications of Molecular Paramagnetism*, ed. E. A. Boudreaux and L. N. Mulay, John Wiley and Sons, New York, 1976.

10 R. Clérac, F. A. Cotton, C. A. Murillo and X. Wang, *Chem. Commun.*, 2001, 205. The methanol solution from which the organometallic dichromium(III,III) compound $Cr_2(\mu\text{-}OMe)_2(\eta^3\text{-}N,C,N'\text{-}H_2DpyF)_2Cl_2$ can be isolated in low yield is red in color.

11 J. Pflugrath and A. Messerschmidt, MADNES, Munich Area Detector (New EEC) System, version EEC 11/1/89, with enhancements by Enraf-Nonius Corp., Delft, The Netherlands. A description of MADNES appears in: A. Messerschmidt and J. Pflugrath, *J. Appl. Crystallogr.*, 1987, **20**, 306.

12 (*a*) W. Kabsch, *J. Appl. Crystallogr.*, 1988, **21**, 67; (*b*) W. Kabsch, *J. Appl. Crystallogr.*, 1988, **21**, 916.

13 F. A. Cotton, R. H. Niswander and J. C. Sekutowiski, *Inorg. Chem.*, 1978, **17**, 3541.

14 See F. A. Cotton, L. M. Daniels, C. A. Murillo, I. Pascual and H.-C. Zhou, *J. Am. Chem. Soc.*, 1999, **121**, 6856 for an in-depth discussion of how various factors affect the Cr–Cr bond length.

15 F. A. Cotton, L. M. Daniels, C. A. Murillo and I. Pascual, *Inorg. Chem. Commun.*, 1998, **1**, 1.

16 F. A. Cotton, L. M. Daniels, C. A. Murillo and H.-C. Zhou, *Inorg. Chim. Acta*, 2000, **305**, 69 and references therein.

17 K. H. Theopold, *Acc. Chem. Res.*, 1990, **23**, 263.